

Higher-order assortativity for directed weighted networks and Markov chains

Alberto Arcagni^a, Roy Cerqueti^{b,c}, Rosanna Grassi^d

^a*MEMOTEF Department, Sapienza University of Rome, Via del Castro Laurenziano, 9, Rome, 00161, Italy*

^b*Department of Economic and Social Sciences, Sapienza University of Rome, Piazzale Aldo Moro, 5, Rome, 00185, Italy*

^c*GRANEM, Université d'Angers, SFR CONFLUENCES, Angers, F-49000, France*

^d*Department of Statistics and Quantitative Methods, University of Milano - Bicocca, Via Bicocca degli Arcimboldi, 8, Milan, 20126, Italy*

Abstract

In this paper, we propose a new class of assortativity measures for weighted and directed networks. We extend Newman's classical degree-degree assortativity by considering node attributes other than degree, and we propose connections among nodes via directed walks of length greater than one, thus obtaining higher-order assortativity. We test the new measure in the paradigmatic case of the world trade network and for other networks from a socioeconomic context, and we also provide some simulation results. Importantly, we show how this global network indicator is strongly related to the autocorrelations of the states of a Markov chain.

Keywords:

Networks, Higher-order Assortativity, Random walks, Markov Chains

1. Introduction

Asymmetric interactions characterize many complex systems in nature, and directed networks are suitable tools for representing these complex situations. However, despite the remarkable persistence of such systems in real-world phenomena, a formal representation as directed networks is still not used, probably because of the difficulty in treating such models mathematically. Indeed, some network indicators are difficult to manage in the directed framework, and some cases lack a proper definition of the network measures for directed networks. Against that background, the focus herein is on providing the generalized concept of an assortativity measure for directed

networks. This theme is relevant because assortativity is a global indicator that provides useful insights about network structure.

In the classical definition by Newman (2002), assortativity is represented by a global measure based on the Pearson correlation between the degrees of nodes. This measure ranges in the interval $[-1, 1]$, having positive values in assortative networks and negative values in disassortative ones. The interpretation of the degree–degree assortativity measure is simple: for undirected networks, high assortativity means that high-degree nodes tend to connect to other high-degree nodes, whereas in disassortative networks, high-degree nodes tend to be connected to low-degree nodes.

The analysis of the correlation between a given attribute of the nodes responds to the necessity to obtain more complete information concerning that provided by the simple distribution of the considered nodal attribute.

The assortativity measure can be extended in two different directions: (i) we can consider quantitative attributes of nodes other than degree, or (ii) we can move on from the adjacency of nodes—which is the basis of Newman’s degree–degree assortativity—and propose more-general ways to connect them. In our approach, we seek to meet both these important requirements. Regarding direction (i), degree-based assortativity provides a restrictive view of the accordance among nodes, but a generalization to different nodal attributes overcomes this issue, extending the meaning of the coefficient to describe similarities and dissimilarities among nodes in terms of something other than degree (Meghanathan, 2016; Arcagni et al., 2019; Yuan et al., 2021). Regarding direction (ii), it is relevant to mention the generalization of Newman’s assortativity index proposed by Arcagni et al. (2017), who provided a closed formula leading to a unifying approach for the assortativity of undirected and unweighted networks. In particular, they considered pairs of vertices not necessarily adjacent but connected via paths, shortest paths, and random walks. Importantly, connecting nodes via paths of length greater than one offers insights into the similarities between connected but non-adjacent nodes. Indeed, high-degree nodes may not be connected directly to each other but nevertheless remain equally connected via low-degree ones.

Arcagni et al. (2017) labeled the new concept of assortativity based on paths as higher-order assortativity, which in particular cases allows us to recover the Newman index as well as other measures based on assortativity (Estrada et al., 2008; Mayo et al., 2015; Van Mieghem et al., 2010) using suitable definitions of the matrix governing the connections. In the same vein, Arcagni et al. (2019) extended higher-order assortativity to a new class of higher-order measures specific for weighted undirected networks, recover-

ing as a particular case the weighted assortativity index introduced by Leung and Chau (2007). The problem of assortativity in directed networks has also been investigated (Yuan et al., 2021). In particular, Foster et al. (2010) and Piraveenan et al. (2010) proposed a natural modification of the Newman formula, encoding the assortativity measure into four directed measures based on combinations of nodal in-degree and out-degree. The coefficients quantify the tendencies of nodes with high in-degree or out-degree to be connected to other such nodes or those with the opposite tendency. However, still lacking is a higher-order measure of assortativity tailored for weighted and directed networks.

This paper contributes by filling this gap. We introduce the new concept of an assortativity measure of order h (with $h \geq 1$) for the general case of weighted and directed networks. According to previous studies and when needed, we refer to this as the higher-order assortativity measure, and we complete the definitions introduced by Arcagni et al. (2017) and Arcagni et al. (2019) by including weighted directed networks. Moreover, the proposed concept is formulated based on a nodal attribute that is not necessarily degree or strength. In doing so, we extend Newman’s assortativity coefficient in both aforementioned directions.

Notice that taking different kinds of centrality measures allows us to have clear information on the similarity of the nodes in terms of other attitudes – like the propensity to create a community (clustering coefficient), the relevance in connecting different sides of the network (betweenness) and so on. Furthermore, the possibility of further generalizing the assortativity measures to the case of directed arcs and also for nodes that are not necessarily adjacent to the reference ones leads to a particularly versatile instrument, to be exploited for the description of the correlations at different levels and according to different attributes.

It is recognized that network-based models can be meaningful for representing the complexity of real-world systems (Gosak et al., 2022; Breza et al., 2019; D’Arcangelis and Rotundo, 2016; Varela and Rotundo, 2016), and studying higher-order properties is particularly relevant. The classical approach of network theory is based on pairwise relationships between nodes, but in real-world networks, interactions between individual entities or groups often go beyond dyadic interactions. This motivates the recent interest in studying interactions that go beyond adjacency relationships. From this perspective, our proposal addresses an essential and relevant issue that will have promising application developments. Interesting published reviews provide an overview of higher-order networks from their mathematical representations to recent advances in this field (Majhi et al., 2022; Bick et al.,

2023).

We show the effectiveness of the proposed measure by applying it to the world trade network. Indeed, network theory provides a good tool for capturing the complexity of trade relations among countries. Several previous studies have been devoted to the structure and dynamics of the international trade network, as well as its connection with fundamental economic factors (Garlaschelli and Loffredo, 2004; De Benedictis and Tajoli, 2011; De Benedictis et al., 2014; Garlaschelli and Loffredo, 2005; Bhattacharya et al., 2008; Acemoglu et al., 2012), and this is why we expect the proposed measure to be useful in this context. We also test the measure on two networks taken from a socioeconomic context, i.e., the electricity trade network and the migration network. Finally, to assess the measure’s sensitivity to variations in model parameters, we apply it to some synthetic networks from a stochastic block model (SBM).

Note that the proposed assortativity measure offers a relevant interpretation in the field of Markov chains (see Norris et al., 1998, for a survey of this class of stochastic processes). Indeed, directed and weighted networks are particularly suitable for describing random flows moving over a discrete set of states identified by nodes. In the graph representation of a Markov chain, the existence of an arc connecting state/node i with state/node j is associated with a non-null probability of jumping from i to j . Therefore, the (suitably normalized) weights of the arcs in a complex network are naturally associated with the probability of observing a flow from a state to another one in the corresponding Markov chain. In stating the bridge between complex networks and Markov chains, we follow the route traced by some relevant contributions in the literature. It is worth mentioning Gómez et al. (2010), who dealt with a disease propagation model by merging complex networks and Markov chains. In the same application environment, Iannelli et al. (2017) elaborated on the informative content of the general network-based measures derived from Markov-chain theory. Our novelty here is to connect higher-order assortativity—a topological property of the network involving nodes other than adjacent ones—and homogeneous discrete-time Markov chains.

Specifically, let us consider nodal assortativity with reference to a given vertex centrality measure. The assortativity index of order h ranges in $[-1, 1]$; it approaches 1 (resp. -1) when the nodes connected via walks of length h have a high level of concordance (resp. discordance) in the considered centrality measure. This variation range suggests that the assortativity index of order h can be interpreted as an autocorrelation term at h lags in the context of Markov chains, and this is exactly our case. Indeed, the order h is

the length of a walk from one node to another, and if we imagine that each link takes one unit of time, then the considered walk takes h units of time. In this respect, the order h can be seen as a temporal variable for a discrete-time Markov chain with states given by the nodes of the network along with their centrality measures and transition probabilities related opportunely to the weights of the network’s links.

This interpretation of the assortativity measure of order h allows us to state a natural bridge between complex networks and stochastic processes. In so doing, we are able to move from the information content of the higher-order assortativity of a network to the dynamical properties of the underlying Markov chain. Specifically, the temporal dimension of the network and the regularities captured by the autocorrelation—which are hidden in the network structure—become clear when moving to Markov-chain theory.

This paper is structured as follows. In Section 2, we describe the mathematical notation, and in Section 3 we introduce the novel definition of higher-order assortativity extended to weighted digraphs. We then apply the proposed index to the world trade network (Section 4) and to the electricity and migration networks (Section 5), and some simulations are shown in Section 6. Section 7 shows how the higher-order assortativity measure can be interpreted in the context of discrete-time homogeneous Markov chains with finite states. Finally, the paper concludes with Section 8.

2. Preliminaries

In this section, we outline some basic definitions and notation related to directed complex networks that are used to present our methodological proposal. For a more detailed treatment, see Bang-Jensen and Gutin (2008), Newman (2010), and Gross and Yellen (2003).

A directed graph (or digraph) $N = (V, A)$ is a pair of sets V and A , where V is the set of n vertices (or nodes) and A is the set of m ordered pairs (arcs) of vertices of V ; if (i, j) and/or (j, i) is an element of A , then vertices i and j are adjacent. An i - j directed walk is a sequence of vertices and arcs from i to j such that all arcs have the same direction.

A weight $w_{ij} > 0$ can be associated with each arc (i, j) so that a weighted digraph is obtained. Moreover, it is assumed that $w_{ij} = 0$ if and only if $(i, j) \notin A$. The w weights are collected in a real n -square matrix \mathbf{W} (the weighted adjacency matrix). By definition, the elements of this matrix describe both the adjacency relationships between the vertices in V and the weights on the arcs. In this context, a weighted directed network is a directed graph $N = (V, A)$ equipped with a weighted non-symmetric matrix \mathbf{W} . In

the unweighted case, non-null weights can take only unitary value, and so matrix \mathbf{W} provides only information about the adjacency relationships. In the case of unweighted networks, we denote \mathbf{W} by \mathbf{A} (the adjacency matrix), and we assume that the principal diagonal of the adjacency matrix is filled by zeros to exclude loops. Indeed, assortativity is usually computed for networks without loops to avoid the trivial situation of computing self-correlations (for example, see the survey on assortativity measures for complex networks by Noldus and Van Mieghem, 2015).

The (i, j) element of the k th power of the matrix \mathbf{A} is the number of directed walks of length k from i to j .

Because in-degree, out-degree, in-strength, and out-strength are the most popular centrality measures in the context of the assortativity, as the original definition by Newman (2002) suggests, we introduce a particular notation for them, along with their definitions. We define the in-degree d_i^I (resp. out-degree d_i^O) of a node $i \in V$ as the number of arcs pointing toward (resp. starting from) i . Then, the in-degree and out-degree vectors are \mathbf{d}^I and \mathbf{d}^O , respectively, and the vector of the vertices' degrees is given by $\mathbf{d} = \mathbf{d}^I + \mathbf{d}^O$. We define the in-strength and out-strength of node $i \in V$ (s_i^I and s_i^O , respectively) and in-strength and out-strength vectors (\mathbf{s}^I and \mathbf{s}^O , respectively) analogously. A vertex $i \in V$ with $d_i^I = 0$ and $d_i^O > 0$ is called a *source* because it is the origin of its outgoing arcs. Similarly, a vertex $i \in V$ with $d_i^O = 0$ and $d_i^I > 0$ is called a *sink* because it is the end of each incoming arc.

3. A novel definition of higher-order assortativity

We consider two vertex centrality measures and collect their values for the weighted directed network N in the n -dimensional vectors \mathbf{x} and \mathbf{y} . We define the higher-order assortativity of length $h \geq 1$ for this weighted digraph as a particular case of the Pearson correlation index in the n -dimensional vectors \mathbf{x} and \mathbf{y} , as follows:

$$r_h = r(\mathbf{x}, \mathbf{y}, \mathbf{E}_h) = \frac{\mathbf{x}^\top (\mathbf{E}_h - \mathbf{p}_h \mathbf{q}_h^\top) \mathbf{y}}{\sqrt{[\mathbf{x}^\top (\mathbf{D}_{\mathbf{p}_h} - \mathbf{p}_h \mathbf{p}_h^\top) \mathbf{x}] [\mathbf{y}^\top (\mathbf{D}_{\mathbf{q}_h} - \mathbf{q}_h \mathbf{q}_h^\top) \mathbf{y}]}} \quad (1)$$

where \mathbf{E}_h is a normalized n -squared matrix whose element in row i and column j is denoted by $e_{ij}^{(h)}$, with $\|\mathbf{E}_h\|_1 = \sum_{i,j=1}^n |e_{ij}| = 1$, while $\mathbf{p}_h = \mathbf{E}_h \mathbf{1}$, $\mathbf{q}_h = \mathbf{E}_h^\top \mathbf{1}$, where $\mathbf{1}$ is the conformable vector of elements equal to 1, and $\mathbf{D}_{\mathbf{p}_h}$ and $\mathbf{D}_{\mathbf{q}_h}$ are the diagonal matrices with the vectors \mathbf{p}_h and \mathbf{q}_h , respectively, on the main diagonal.

$Cov(\mathbf{x}, \mathbf{y}, \mathbf{E}_h) = \mathbf{x}^\top (\mathbf{E}_h - \mathbf{p}_h \mathbf{q}_h^\top) \mathbf{y}$ is the covariance between \mathbf{x} and \mathbf{y} with joint distribution \mathbf{E}_h , $Var(\mathbf{x}, \mathbf{p}_h) = \mathbf{x}^\top (\mathbf{D}_{\mathbf{p}_h} - \mathbf{p}_h \mathbf{p}_h^\top) \mathbf{x}$ is the variance of \mathbf{x} with distribution \mathbf{p}_h , and $Var(\mathbf{y}, \mathbf{q}_h) = \mathbf{y}^\top (\mathbf{D}_{\mathbf{q}_h} - \mathbf{q}_h \mathbf{q}_h^\top) \mathbf{y}$ is the variance of \mathbf{y} with distribution \mathbf{q}_h .

In particular, we assume that $\mathbf{E}_1 = \frac{\mathbf{W}}{\|\mathbf{W}\|_1}$, and as we will see in Section 7.2, matrix \mathbf{E}_h is also related to Markov chains for all $h \geq 1$. Therefore, the assortativity measure in Eq. (1) depends on suitable centrality measures \mathbf{x} and \mathbf{y} that are related to the initial and terminal state, respectively, of a stochastic process of h steps.

The considered higher-order assortativity extends the related concepts introduced by Arcagni et al. (2017, 2019) for weighted undirected networks. In accord with Newman (2002), we note that the in-strength and out-strength of the nodes play a relevant role when dealing with assortativity also in the context of weighted digraphs. Indeed, such centrality measures provide distinct information about the network topology. Therefore, we describe such cases in detail while also giving the interpretation of the higher-order assortativity measure in this particular context.

Specifically, for a complete treatment of the higher-order assortativity measure for weighted and directed networks, we consider all possible combinations of in-strength and out-strength, and starting from Eq. (1), we define the four types of higher-order assortativity index for weighted digraphs as follows.

1. $r_h^{OI} = r(\mathbf{s}^O, \mathbf{s}^I, \mathbf{E}_h)$ (out-in)

This coefficient evaluates the correlation between the out-strength and in-strength vectors using Eq. (1) for nodes that are connected via a directed walk of length h . Specifically, a high value of r_h^{OI} is associated with high concordance between the out-strength and in-strength of such vertices, while a value of r_h^{OI} close to -1 implies high discordance.

2. $r_h^{IO} = r(\mathbf{s}^I, \mathbf{s}^O, \mathbf{E}_h)$ (in-out)

This index measures the concordance and discordance between the in-strength of the starting vertices and the out-strength of the arrival vertices after a directed walk of length h .

3. $r_h^{II} = r(\mathbf{s}^I, \mathbf{s}^I, \mathbf{E}_h)$ (in-in)

This coefficient provides an evaluation of the correlation between the in-strength of the starting vertices and the in-strength of the ending vertices in the presence of a directed walk of length h .

4. $r_h^{OO} = r(\mathbf{s}^O, \mathbf{s}^O, \mathbf{E}_h)$ (out-out)

This version of the higher-order assortativity index captures the correlation between the out-strength of the starting vertices and the out-

strength of the terminal ones when they are connected via a directed walk of length h .

Note that given h , it is not necessarily the case that $r_h^{OI} = r_h^{IO}$ because the indexes depend on the distribution of directed walks described by the matrix \mathbf{E}_h , which is not necessarily symmetric.

4. Higher-order assortativity in the world trade network

To illustrate the advantages of our definition, we show an application of higher-order assortativity to the world trade network. This application is interesting given the extensive literature merging networks and economic theory (see Carvalho and Tahbaz-Salehi, 2019, for an excellent review of the literature on production networks from both theoretical and empirical perspectives).

International trade plays a fundamental role in the global economic system, and understanding the structure of interactions among economic agents at the international level is useful for studying the cross-country transmission and propagation of local shocks (Acemoglu et al., 2012; Carvalho, 2014; Acemoglu et al., 2016) or for explaining the co-movement of business cycles (Long and Plosser, 1983; Burstein et al., 2008). In this context, complex networks and their properties are effective in offering a way to represent these interactions. In this regard, some interesting contributions are those by Serrano et al. (2007), De Benedictis and Tajoli (2011), De Benedictis et al. (2014), Fagiolo et al. (2008), Barigozzi et al. (2010), and Bartesaghi et al. (2022). One property of the trade network is the local heterogeneity of its structure (Serrano et al., 2007; De Benedictis and Tajoli, 2011). Fagiolo et al. (2008) showed the coexistence of weak and strong trade links, and countries with intense trade relationships tend to be more clustered together. Acemoglu et al. (2012) studied how the intersectoral network structure contributes to generate aggregate fluctuations from microeconomic shocks. The empirical model of network formation proposed by Mundt (2021) applied to the input–output data reveals significant fluctuations of network ties over time, inducing changes also in the aggregate network structural properties.

Studying higher-order assortativity for the trade network is motivated by the complexity of the trade relationships, which often cannot be explained by simply investigating adjacent commercial partners, and the higher-order properties of the network could be more informative than the first-order ones. For instance, Acemoglu et al. (2012) stated that even if two different networks exhibit the same first-order characteristics (same degree or strength

distribution), different higher-order interactions among economic sectors can lead to different levels of severity of aggregate downturns. These facts motivate us to test our measure on the world trade network.

The data refer to goods traded between countries, with the trade volumes expressed in US dollars¹. We constructed both export and import weighted networks, where the vertices are countries and the weights on arcs represent the volumes of imported or exported goods among 222 countries in the year 2021. Note that the number of vertices is greater than the number of recognized countries because ComTrade includes even almost-uninhabited territories. Therefore, in the following, the word “country” covers a broad definition that also includes these regions.

Concerning links between countries, the export network should be complementary to the import network because import from i to j should be equal to export from j to i . However, this is not the case because the data describe only trade declared officially by *reporter* countries with their *partners*, and some declarations are either missed or mismatched. This problem pertains also to years before 2021.

Here, we follow an approach similar to that adopted by Antonietti et al. (2022), who constructed a symmetric trade network aggregating import and export data. However, unlike Antonietti et al. (2022), our network preserves the edge directions, working in this way with a directed network.

More specifically, let \mathbf{W}_I and \mathbf{W}_E be weighted adjacency matrices representing the volumes of import and export trade among countries. Thus, the trade network is defined as $N = (V, \mathbf{W})$, where the elements w_{ij} of the matrix \mathbf{W} are

$$w_{ij} = \max(w_{ij}^E, w_{ji}^I),$$

with w_{ij}^E and w_{ji}^I being the ij entries of matrices \mathbf{W}_E and \mathbf{W}_I^T , respectively. In this way, the asymmetric matrix \mathbf{W} expresses the flow of goods from country i to country j . Note that in constructing \mathbf{W} , we choose the maximum between import and export. Indeed, in line with Antonietti et al. (2022), we assume that the higher the value declared, the higher the quality of the information that can be contained.

4.1. Analysis of main characteristics of network

First, we analyze some classical network characteristics. The number of vertices is $n = 222$, and let \mathbf{A} be the adjacency matrix obtained from \mathbf{W}

¹The data are freely available for download from ComTrade; see UN COMTRADE (2022).

by neglecting the arc weights. The network *density* is computed as the ratio between the total number of arcs and the maximum number of potential arcs² $n(n - 1)$. Therefore, the density is

$$\frac{\|\mathbf{A}\|_1}{n(n - 1)} = \frac{\sum_{i,j=1}^n a_{ij}}{n(n - 1)} = 0.4996.$$

Although one might expect the trade network to be complete, this is not so in this case because of the presence of peripheral nodes representing small countries and regions that probably communicate only a part of their exports or imports.

Distributions of centrality measures—in particular degree and strength—provide other important information. The degree and strength of a vertex represent the number and volume of a country’s exchanges, giving insights into the diversification and intensity of trade. Fig. 1 shows the marginal distributions of in–out degree and in–out strength. In line with Bhattacharya et al. (2008), in-strength and out-strength are represented graphically using a logarithmic scale with base 10. We choose the log-transformation for the strength because in the trade network, the strength increases exponentially and the resulting distribution is log-normal. In fact, as can be seen in Fig. 1, the log-strength has a bell shape similar to that of a normal distribution. Choosing a logarithmic base equal to 10 allows us to express the scale of trade in multiples of ten thousand million dollars.

The distributions of the “in” and “out” measures are quite similar, but note the following characteristics of the degree and log-strength distributions: (i) on the horizontal axis, the magnitude of the degree corresponding to the number of countries is a few hundred, whereas that of the strength ranges from 10^6 to 10^{12} ; (ii) the log-strength distribution is bell-shaped; (iii) the degree distribution is polarized because more than half of the countries have connections with fewer than 100 other countries, while one-tenth of the countries are connected with almost all the other ones. As we will see later, this last characteristic is meaningful when searching for clusters of central and peripheral countries.

We now compare countries via the four centrality measures: in-degree, out-degree, in-log-strength, and out-log-strength. Table 1 shows the strong correlations (computed using the Pearson coefficient) between the considered variables. As expected, the “in” and “out” directions are strongly correlated (0.883 and 0.947 for degree and log-strength, respectively). However, there is

² N is a directed network without loops.

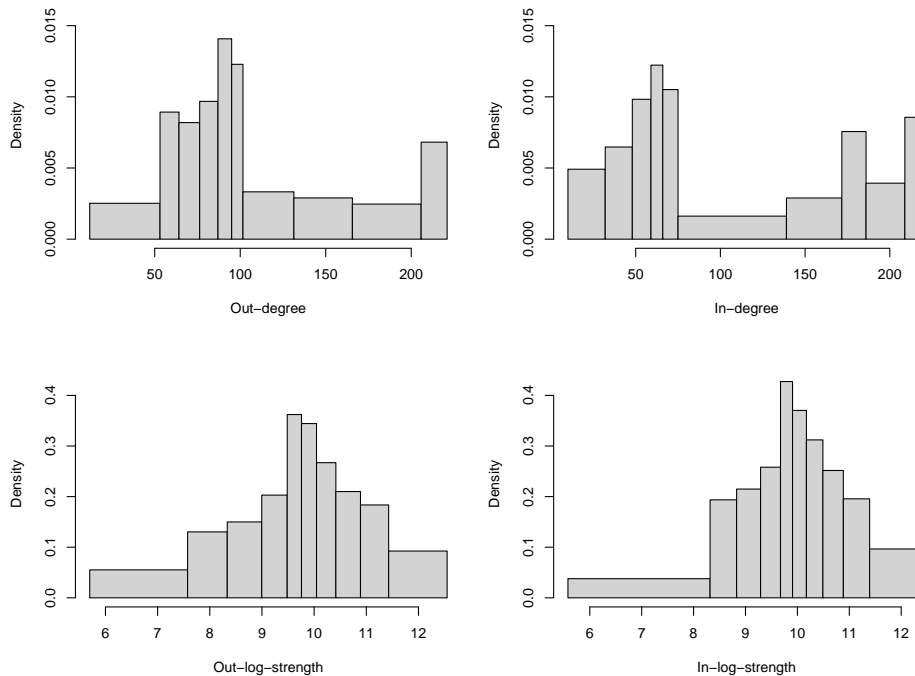


Figure 1: Histograms of four centrality-measure distributions observed on 222 countries. The distributions are partitioned into 10 classes whose breaks are the deciles, and the heights of the rectangles are the densities of the relative frequencies, so each rectangle represents about one-tenth of the observations. The top-left histogram represents the out-degree distribution, the top-right one the in-degree distribution, the bottom-left one the out-log-strength distribution, and the bottom-right one the in-log-strength distribution.

also a strong *linear* correlation between degree and log-strength centralities, with values ranging from 0.771 to 0.792. Although correlation is not causation, these high values suggest that an increasing number of connections increases volumes exponentially.

We now analyze the principal components from the standardized variables. The first component represents 87% of the whole variability (considering the first two together, the variability increases to 96%), and its loading is all positive. Therefore, its scores can be used to provide a mixed and rough order of the countries in terms of centrality. In increasing order, the top 10 central countries are Canada, Belgium, Japan, Italy, Great Britain, the Netherlands, France, Germany, China, and the United States.

We performed a hierarchical cluster analysis using the four principal com-

	in-deg.	out-deg.	in-log-str.	out-log-str.
in-deg.	1			
out-deg.	0.883	1		
in-log-str.	0.792	0.785	1	
out-log-str.	0.742	0.771	0.947	1

Table 1: Matrix of correlations between centrality measures.

ponents instead of the strongly correlated original variables. We used Euclidean distances between countries, and we defined distances between groups with the complete method. The number of groups suggested by the hierarchical method is two. One cluster of 116 is composed of small territories and countries almost peripheral in terms of trade volumes, and the other cluster of the remaining 106 countries controls most of the volumes; we refer to the latter cluster as the main network.

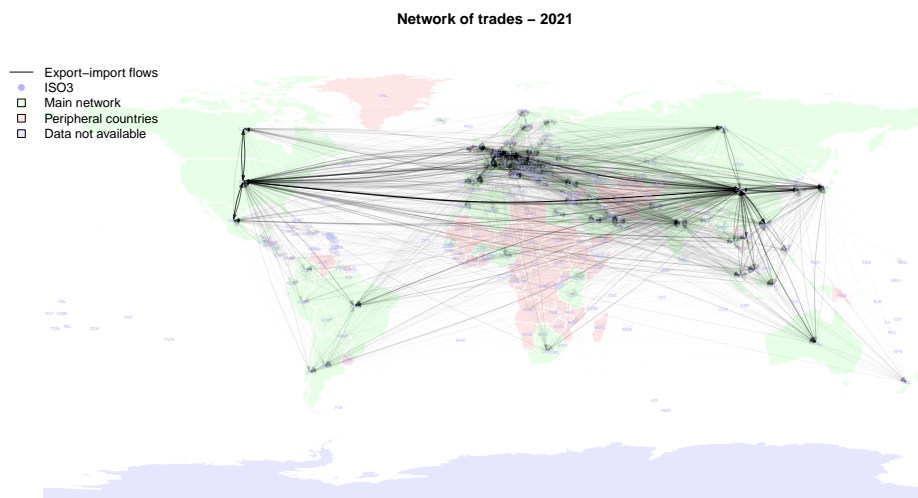


Figure 2: Map of world trade network. A directed edge is represented by a black arrow from the exporting country to the importing one, the opacity of which is proportional to the value of the traded goods. Countries are clustered via a hierarchical division method using the centrality measures (in and out degree and log-strength) as the original dimensions. The optimal cutting of the dendrogram generates two groups that can be interpreted as the main network (green) and peripheral countries (red).

Fig. 2 provides a graphical representation of the trade network, showing the groups that emerged from the cluster analysis, i.e., the main network

and peripheral countries. However, how these groups relate to each other remains to be investigated. As we will see in the next subsection, assortativity provides an answer in terms of centrality correlation.

4.2. Higher-order assortativity

Evidently, there are several combinations of centrality measures and adjacency matrices that can be used when computing the higher-order assortativity coefficient. In this section, we focus on only those cases that offer a more intuitive interpretation of the results in the context of the world trade network³.

It is important to note that the assortativity coefficient can be developed by taking the centrality measures \mathbf{x} and \mathbf{y} as in- or out- one, as explained in the four cases of assortativity in Section 3 (in-out, out-in, in-in, out-out). The selection of \mathbf{x} and \mathbf{y} leads to different assortativity measures with different interpretations. In particular, we give the following economical interpretations of the used centrality measures: out-going centrality measures supply, i.e., the out-degree and out-strength of vertex i reflect the supply of goods of country i ; in-going centrality measures demand, i.e., the in-degree and in-strength of vertex i reflect the demand of goods of country i ; the directions of edges represent export, i.e., an arrow from i to j represents export from country i to country j .

In view of the economic meanings of the centrality measures given above, the most suitable directed assortativity in this application is the out-in assortativity r_h^{OI} in order to effectively track the paths of the exchanges of goods between countries. Indeed, referring to the volume of flows (then to the strength), of the four measures proposed herein, those mentioned above describe well the relationship between exporting and importing countries.

Fig. 3 shows the higher-order direct assortativity for increasing h computed on both the unweighted and weighted network. In both cases, the network is disassortative at order $h = 1$, which means that the exporters with many connections and a large volume tend to trade with small importers. Note that in absolute value, the assortativity is always lower than 0.5, which is because of large traders needing to trade with each other (e.g. the United States and China) and maybe also small traders.

At order $h = 2$ the assortativity becomes positive. Similar behavior has also been observed for undirected networks (Arcagni et al., 2017, 2019), and it

³We also computed the higher-order assortativity measures in all the remaining cases and results are available upon request.

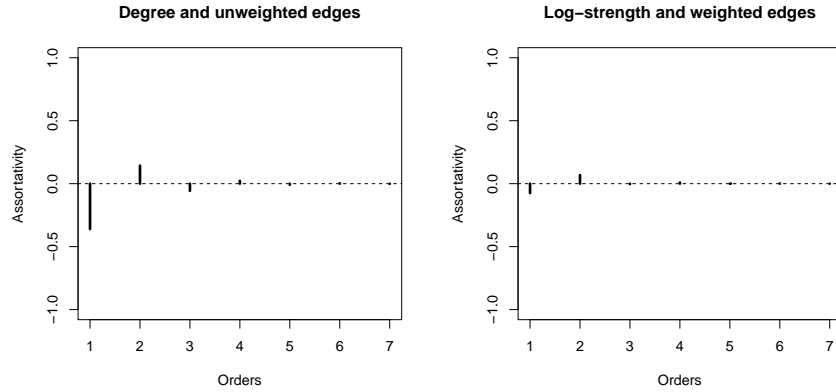


Figure 3: Higher-order assortativity between out-centrality and in-centrality of world trade network; results refer to unweighted structure (left) and weighted network using log-strength as centrality measure (right); x-axis represents the length of walks, y-axis the assortativity indexes.

may be the consequence of the disassortative behavior at order $h = 1$. Indeed, if at the first step exporters and importers tend to belong to different groups, then at the second step they tend to belong to the same one. Focusing on the meaning of the measure, because the network refers to the totality of traded goods, the exchange of goods between countries i and k may occur directly (e.g. exchanging raw materials) in one time unit $h = 1$ or indirectly in two time units $h = 2$ through the transformation of the raw materials (into semi-manufactured goods) via country j . Then, the assortativity of order $h = 2$ captures a new pattern of the exchange of goods between two countries. This bouncing between disassortative and assortative behavior continues for odd and even orders, respectively.

Considering the weights, the behavior of higher-order assortativity is similar because of the correlations among centrality measures reported in Table 1. However, considering the weights, we observe a strong reduction in the amplitude of variation. In fact, weights on arcs separate the main network (identified with the cluster analysis) from the remaining, and the main network of trades is almost complete as expected.

Finally, we observe that assortativity tends to zero when the order increases, this being because of the increased randomness in the expected flow of goods in the network.

5. Other applications

In this section, we apply our indexes to two different real-world networks in order to show the effectiveness of the proposed measure in other contexts as well. The considered networks are the electricity trade network and the migration network. This allows us to provide different results and to investigate the long-term behavior of people flows or a specific sector in the trade scenario.

5.1. Electricity trade network

Unlike the application to the world trade network, in which the total volume of trade was considered, we focus here on the specific electricity sector. Also, in this case weights refer to the value and are expressed in US dollars.

In the analysis, we are interested in the exchanges between countries, therefore the electricity produced for self-consumption is not included; formally, the network construction does not incorporate loops. From an economic perspective, this implies that trade is concentrated mainly in Europe, with China and the United States becoming peripheral countries in the network. Unlike the whole trade network that incorporates the aggregated volume of traded goods, this network has only 10 source nodes (then zero in-centrality) and 29 sinks (then zero out-centrality). Therefore, the weighted results are based on the strength centrality because the log-strength is not finite.

Fig. 4 shows the results, and it is evident that the outcomes are quite different from those in the case of the whole trade network. This is due to the different network topology that emerges when we focus on only this specific sector. In this case, some countries (e.g., the United States) self-produce electricity for internal consumption, which can have more than one motivation. For instance, it is related to a country's investment in renewable energies. In this sense, the United States does not follow a general common regulation as in Europe, and investment in renewable energies is left as a choice of individual states, some of which are experimenting with beneficial forms of energy self-production. Conversely, European countries are in general still dependent on energy supplied from external sources (Di Silvestre et al., 2021). Therefore, trade is concentrated mostly in Europe, and European countries have high centrality. Consequently, the assortativity is always positive and seems not to vanish.

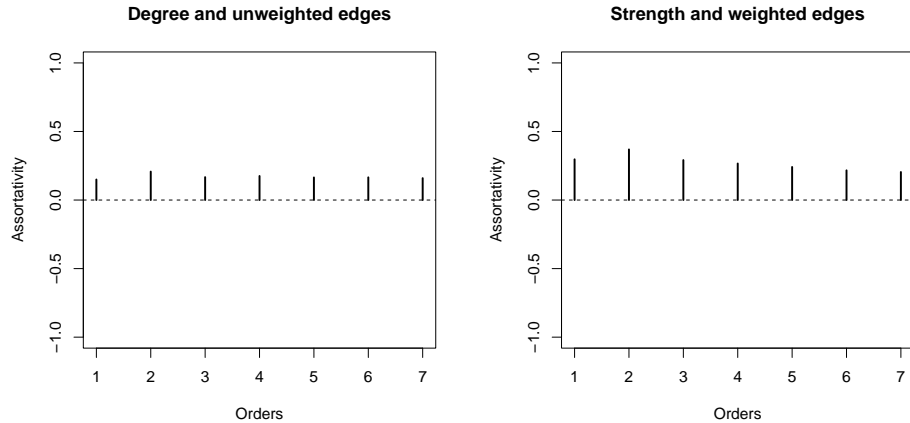


Figure 4: Higher-order assortativity between out-centrality and in-centrality of electricity trade network. The results refer to the unweighted structure (left) and the weighted network using strength as the centrality measure (right). The horizontal axis represents the walk length, and the vertical axis represents the assortativity index.

5.2. International migration network

In this application, a network of people is constructed starting from the international migration database provided by OECD (2020)⁴, which is the most recent and complete dataset. Weights correspond to the number of migrants in a year from a country to another one.

Similar to the world trade network, two information items are available for each pair of countries: the number of outgoing people, and the number of incoming people. As was done in the case of the international trade network, we assume as weights the largest numbers of people, and we preserve the edge directions.

Fig. 5 shows the higher-order assortativity indexes obtained for this application. The international migration network is disassortative for walks of odd length and assortative for walks of even length. At order $h = 1$, both the binary and weighted networks exhibit disassortative behavior, and this is in line with the literature (Fagiolo and Mastrorillo, 2013). Finding the actual reason for the oscillating behavior of the assortativity measure would require migration to be explored in depth, which is well beyond the present scope, but we can make some interesting suggestions. For various reasons

⁴<https://stats.oecd.org/Index.aspx?DataSetCode=MIG#>

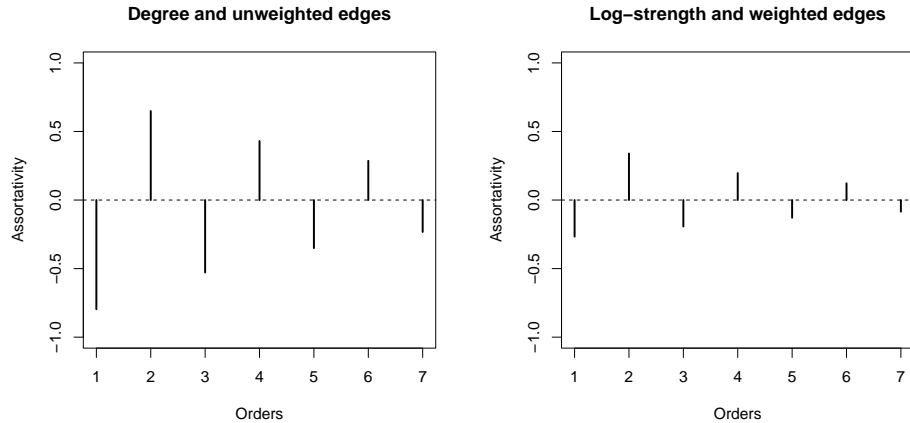


Figure 5: Higher-order assortativity between out-centrality and in-centrality of network based on International Migration Database. The results refer to the unweighted structure (left) and the weighted network using log-strength as the centrality measure (right). The horizontal axis represents the walk length, and the vertical axis represents the assortativity index.

(e.g., geographical), few countries are typically the first destination of people coming from many poor countries, and often the first country reached is only the first step of a long journey, with the final destination reached after passing through different intermediate countries. For instance, several countries with low migrations outflows concentrate migrants toward a few countries with high levels of inflow (e.g., the European countries that are closer to the migration source). As a second step, migrants disperse into Europe, moving to several countries with low levels of inflow. This fact is reflected by the alternating behavior of the assortativity as the order increases. The results based on the weighted network replicate the unweighted structure but with smaller absolute values.

6. Simulations

In this section, some simulations are reported to show how the assortativity at a few steps is strongly conditioned by the weights.

Figs. 6 and 7 show 500 simulated networks from an SBM for different network sizes $n \in \{20, 50, 100, 200, 500, 1000\}$. The same simulations were proposed by Yuan et al. (2021) for the case of assortativity of order $h = 1$. The results in Fig. 6 refer to binary networks, in which case the higher-order indexes are computed by identifying the node degree as the centrality

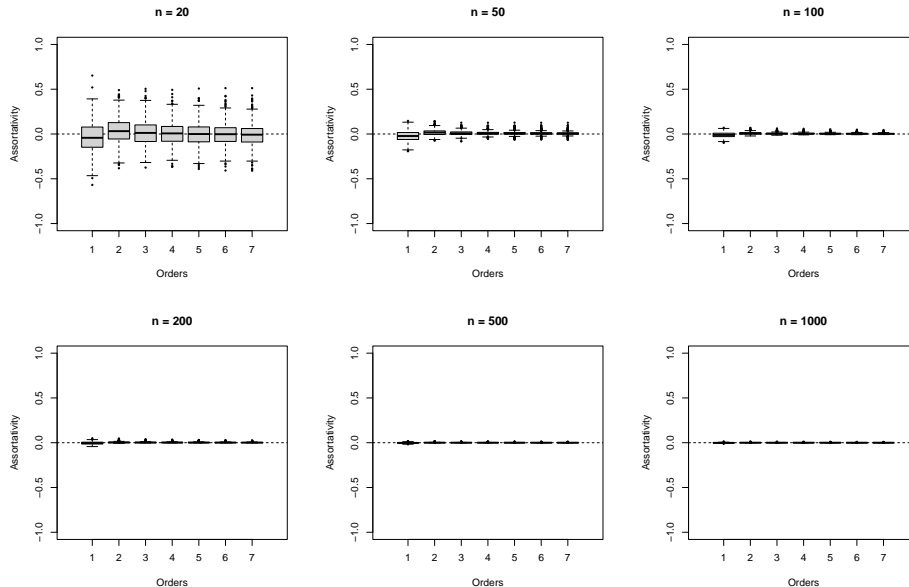


Figure 6: Higher-order assortativity between out-degree and in-degree using binary adjacency matrix of 500 simulated networks from stochastic block model (SBM) comparing different sizes n of the model. The horizontal axis represents the walk length, and the vertical axis represents the assortativity index. The simulations returned different distributions of the assortativity index for each order, so the distributions are represented using box plots to show the quartiles and any anomalous values.

measure and using the binary adjacency matrix to build the matrix \mathbf{E} . In Fig. 7, the results refer to weighted networks, in which case the strength is adopted as the centrality measure and the weighted adjacency matrix is used to build the matrix \mathbf{E} . The simulation results are represented by box plots depicting the distribution of the results for different orders h . To provide an intuitive view of matrices \mathbf{E}_h , we show the case of $h = 1, \dots, 20$ for a simulated Erdős–Rényi directed network with order $n = 100$ (see the Supplementary material).

The simulations were run under the same conditions as those of Yuan et al. (2021). The SBM comprises blocks of Erdős–Rényi directed graphs with probability p of creating an arc within blocks. An edge between two blocks is generated with probability $p' < p$. Because the networks are directed, once an edge is created, a direction is assigned to that edge with equal probability 0.5. In line with Yuan et al. (2021), we consider two blocks, each

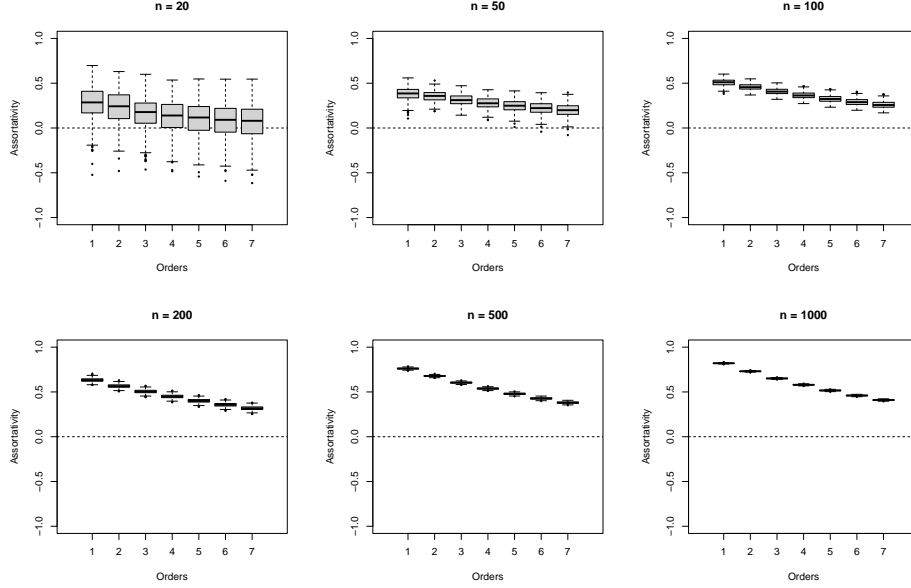


Figure 7: Higher-order assortativity between out-strength and in-strength using weighted adjacency matrix of 500 simulated networks from SBM comparing different sizes n of the model. The horizontal axis represents the walk length, and the vertical axis represents the assortativity index. The simulations returned different distributions of the assortativity index for each order, so the distributions are represented using box plots to show the quartiles and any anomalous values.

with the same size $n/2$, the within probability is $p = 0.2$, and the between probability is $p' = 0.02$. Weights are also assigned as in the cited article: the first block has weights sampled uniformly from integers between 0 and 5, the second block has weights sampled uniformly from integers between 5 and 10, and arcs between blocks have weights equal to 5.

The networks with sizes 20 and 50 show many outliers. However, in both the unweighted and weighted cases, the stability of the simulations increases with the network size. Focusing on the weighted case, the first block is characterized by vertices with low centrality and the second one by vertices with high centrality. Because the within probability p is much higher than the between probability p' and the two blocks are characterized by different levels of weights, there are more connections between vertices with similar centrality. In other words, the walk remains trapped in the block and struggles to exit from it.

In the unweighted case, the assortativity is close to zero because the two blocks have the same structure; this is typical of an Erdős–Rényi game, which generates almost regular graphs with a low variability in degree. On the contrary, when taking the weights into account, the assortativity is positive because nodes tend to be connected to others with the same strength but not to those with different strengths. This is because the probability of creating edges within blocks is higher than that of creating them between blocks. The strength has different expected values but the same variability in each block. The simulations for the unweighted case required almost an hour, and the time was similar for the weighted case.

To enable the simulations to be reproduced, we have provided the R code for weighted networks in the supplementary material. In the unweighted case, it is sufficient to remove the instructions that assign weights to the edges. Note that most of the R instructions are related to the simulation of the SBM, and the higher-order assortativity is computed with only one instruction thanks to the `H0asso` package that evaluates the assortativity for objects of class `igraph` from the homonym package (Csardi and Nepusz, 2006; Csárdi et al., 2023).

7. A Markov chains-based interpretation of the higher-order assortativity

In this section, we formalize the informative content of the higher-order assortativity measure in terms of the transition probabilities of discrete-time homogeneous Markov chains with finite states. As a premise, we introduce some basic definitions and notation for Markov chains. For a complete treatment, see Norris et al. (1998).

7.1. Markov chains: basic definitions and notation

A homogeneous discrete-time Markov chain with finite states is a stochastic process $\mathcal{X} = (X(t) : t \in \mathbb{N})$ such that the following conditions are true.

(P1) There exists a set V with n elements such that $X(t) \in V$ for each $t \in \mathbb{N}$. The elements of V are the states of \mathcal{X} , and the set V is the state space of the Markov chain.

(P2) The Markov property holds, i.e.,

$$P(X(t+1) = j | X(t) = i, X(t-1) = i_{t-1}, \dots, X(0) = i_0) = P(X(t+1) = j | X(t) = i),$$

for each $t \in \mathbb{N}$ and $i, j, i_0, \dots, i_{t-1} \in V$.

(P3) The one-step transition probabilities are invariant with respect to time, i.e.,

$$P(X(t+1) = j | X(t) = i) = P(X(1) = j | X(0) = i),$$

for each $t \in \mathbb{N}$ and $i, j \in V$. We collect all the one-step transition probabilities in an n -square matrix \mathbf{P} whose generic element is $p_{ij} = P(X(1) = j | X(0) = i)$. \mathbf{P} is the transition probability matrix of the Markov chain \mathcal{X} .

As we will see below, the node set V of the network coincides with the state space of the Markov chain.

Properties (P1)–(P3) allow us to identify a Markov chain via three elements: the state space V , the transition probability matrix \mathbf{P} , and the initial probability distribution $\pi_0 = (\pi_0(1), \dots, \pi_0(n))$, where $\pi_0(i) = P(X(0) = i)$ for each $i \in V$. In particular, property (P3) states that the Markov chain \mathcal{X} is homogeneous.

Furthermore, property (P3) can be extended to the case of h -step transition probabilities that are invariant with respect to time for each $h \in \mathbb{N}$. A straightforward computation shows that

$$P(X(t+h) = j | X(t) = i) = P(X(h) = j | X(0) = i) \quad (2)$$

for each $t, h \in \mathbb{N}$ and $i, j \in V$. We collect the h -step transition probabilities in the n -square matrix \mathbf{P}_h , the element of which in row i and column j is $p_{ij}^{(h)} = P(X(h) = j | X(0) = i)$.

Because the state space V is finite, the matrix \mathbf{P}_h is \mathbf{P}^h , i.e., the h -step transition probability matrix is the h th power of the one-step matrix \mathbf{P} .

7.2. Higher-order assortativity in the context of Markov chains

Given $h \geq 1$, we recall that $\|\mathbf{E}_h\|_1 = 1$. Therefore, by referring to Markov-chain theory, the generic element $e_{ij}^{(h)}$ may represent the joint probability that i and j are the position states of \mathcal{X} at time t and $t+h$, respectively, for each t , i.e.,

$$e_{ij}^{(h)} = P(X(h) = j, X(0) = i). \quad (3)$$

By considering the Markov chain \mathcal{X} for which Eq. (3) is true and by using the conditioned probability definition, we can write

$$\mathbf{E}_h = \mathbf{D}_{\pi_0} \mathbf{P}^h, \quad (4)$$

where \mathbf{D}_{π_0} is a diagonal n -squared matrix whose diagonal entries are the components of the initial distribution π_0 .

Notice that (4) leads to $\mathbf{E}_1 = \frac{\mathbf{W}}{\|\mathbf{W}\|_1} = \mathbf{D}_{\pi_0} \mathbf{P}$. Thus, matrices \mathbf{D}_{π_0} and \mathbf{P} identify \mathbf{E}_h , for each $h \geq 1$. In this respect, we notice that the construction of \mathbf{E}_h is not flexible, being constrained to the considered network. This said, we do not have any conditions on the selection of the network, so that we have the possibility of representing \mathbf{E}_h in the case of any chosen structure.

From matrix \mathbf{P} and then \mathbf{P}^h with $h > 1$, which is stochastic by rows, i.e., the rows of the matrix sum to 1, we have $\mathbf{P}^h \mathbf{1} = \mathbf{1}$ and hence

$$\mathbf{E}_h \mathbf{1} = (\mathbf{D}_{\pi_0} \mathbf{P}^h) \mathbf{1} = \mathbf{D}_{\pi_0} (\mathbf{P}^h \mathbf{1}) = \mathbf{D}_{\pi_0} \mathbf{1} = \pi_0, \quad (5)$$

which gives $\pi_0 = \mathbf{p}_h$, $h \geq 1$, where \mathbf{p}_h is the vector that appears in Eq. (1). Indeed, given joint probabilities $e_{ij}^{(h)}$, by Eq. (3) we have

$$\sum_{j=1}^n e_{ij}^{(h)} = \sum_{j=1}^n P(X(h) = j, X(0) = i) = P(X(0) = i) = \pi_0(i) \forall i = 1, \dots, n,$$

i.e., \mathbf{p}_h is the initial probability distribution.

It is clear that in general there is no unique Markov chain \mathcal{X} with state space V for which Eq. (4) is valid. However, given Eq. (5), there is a unique vector π_0 . So, once we choose the network $N = (V, A)$, there is a unique Markov chain $\mathcal{X} = (X(t) : t \in \mathbb{N})$ with V, \mathbf{P} , and π_0 fixed.

Note that for each network node $i \in V$ that is a sink, matrix \mathbf{P} must be stochastic. Therefore, a 1 is added in the main diagonal to associate with the sink an absorbing state in the Markov chain, and $\pi_0(i)$ must be 0 so as not to modify the network topology and comply with Eq. (4) for $h = 1$. On the contrary, $\pi_0(i) > 0 \forall i \in V$ if i is not a sink because then Eq. (4) returns a zero line in \mathbf{E}_1 no matter the values in \mathbf{P} .

Analogous to Eq. (5), we have

$$\mathbf{E}_h^\top \mathbf{1} = (\mathbf{D}_{\pi_0} \mathbf{P}^h)^\top \mathbf{1} = (\mathbf{P}^h)^\top \mathbf{D}_{\pi_0} \mathbf{1} = (\mathbf{P}^h)^\top \pi_0 = \pi_h \quad (6)$$

then $\pi_h = \mathbf{q}_h$, $h \geq 1$, where \mathbf{q}_h is the vector that appears in Eq. (1). Again, by Eq. (3) we have

$$\sum_{i=1}^n e_{ij}^{(h)} = \sum_{i=1}^n P(X(h) = j, X(0) = i) = P(X(h) = j) = \pi_h(j) \forall j = 1, \dots, n,$$

i.e., \mathbf{q}_h is the probability distribution after h steps.

Keeping this in mind, we can rewrite the higher-order assortativity index (defined in Eq. 1) in the Markov-chain context as

$$r_h = r(\mathbf{x}, \mathbf{y}, \mathbf{D}_{\pi_0} \mathbf{P}^h) = \frac{\mathbf{x}^\top (\mathbf{D}_{\pi_0} \mathbf{P}^h - \pi_0 \pi_h^\top) \mathbf{y}}{\sqrt{[\mathbf{x}^\top (\mathbf{D}_{\pi_0} - \pi_0 \pi_0^\top) \mathbf{x}] [\mathbf{y}^\top (\mathbf{D}_{\pi_h} - \pi_h \pi_h^\top) \mathbf{y}]}}. \quad (7)$$

The higher-order assortativity index of length h then represents the auto-correlation at time-distance h of a Markov chain evaluated not on the states $v_i \in V$ but on their transformations \mathbf{x} and \mathbf{y} . Indeed, in a network context, centrality measures can be the image of a real function on the node set V .

7.3. Some illustrative examples

We present some toy examples to illustrate how the newly introduced assortativity measure works in the context of Markov chains. For this, we consider some instances of weighted networks whose related Markov chains have a meaningful state classification. We go into detail below.

We consider four networks $N_k = (V, \mathbf{W}_k)$ with $k = 1, \dots, 4$, sharing the same set of nodes $V = \{a, b, c, d, e\}$ and with weighted adjacency matrices \mathbf{W}_k defined as follows:

$$\mathbf{W}_1 = \begin{pmatrix} 0 & 2 & \mathbf{2} & 2 & 0 \\ 396 & 0 & 0 & 4 & 0 \\ 0 & 0 & 0 & 0 & 0 \\ 0 & 4 & 0 & 0 & 396 \\ 0 & 2 & \mathbf{2} & 2 & 0 \end{pmatrix}, \quad \mathbf{W}_2 = \begin{pmatrix} 0 & 2 & \mathbf{196} & 2 & 0 \\ 396 & 0 & 0 & 4 & 0 \\ 0 & 0 & 0 & 0 & 0 \\ 0 & 4 & 0 & 0 & 396 \\ 0 & 2 & \mathbf{196} & 2 & 0 \end{pmatrix},$$

$$\mathbf{W}_3 = \begin{pmatrix} 0 & \mathbf{2} & 198 & 0 & 0 \\ 0 & 0 & 0 & 100 & 0 \\ 150 & 0 & 0 & 0 & 150 \\ 0 & 200 & 0 & 0 & 0 \\ 200 & 0 & 200 & 0 & 0 \end{pmatrix}, \quad \mathbf{W}_4 = \begin{pmatrix} 0 & \mathbf{198} & 198 & 0 & 0 \\ 0 & 0 & 0 & 100 & 0 \\ 150 & 0 & 0 & 0 & 150 \\ 0 & 200 & 0 & 0 & 0 \\ 200 & 0 & 200 & 0 & 0 \end{pmatrix}.$$

The networks are shown in Fig. 8. From inspection, note that N_1 and N_2 have the same topology and differ only by two weights. In particular, there are no outflows from node c ; i.e., it is a sink. However, while in the former case the inflows into node c have remarkably low weights, in the latter they are particularly high. This evidence is true in terms of the weights' absolute values (i.e., considering matrices \mathbf{W}_1 and \mathbf{W}_2) but also from a relative perspective (i.e., considering the transition probability matrices \mathbf{P}_1 and \mathbf{P}_2 shown below).

Also, N_3 and N_4 share the same topology, and there are no outflows from the class of nodes $\{b, d\} \subset V$. In both cases, it is possible to have an inflow in such a class from the set $\{a, c, e\}$ via the arc from node a to node b . This arc has a low weight in network N_3 but a remarkably high one in N_4 .

We now consider the centrality measures. In Table 2, we report the in-strength \mathbf{s}_k^I and out-strength \mathbf{s}_k^O distributions for each network N_k , $k = 1, \dots, 4$ as well the average values. Note that the average values for the in-strengths and out-strengths are the same because of the associativity of the sum.

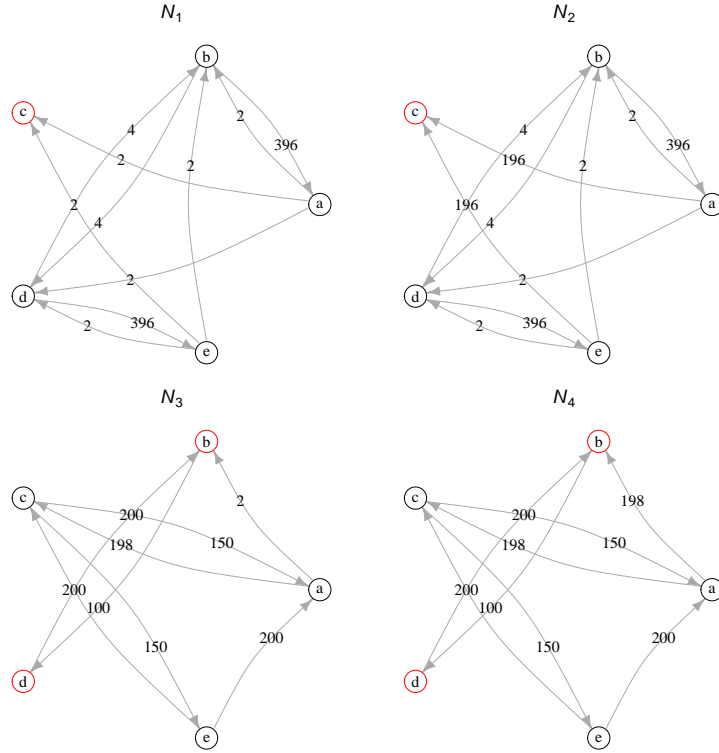


Figure 8: Graphical representations of four illustrative examples. The red vertices are sinks or classes without out-flows. The numbers on the edges refer to the corresponding weights. Networks N_1 and N_2 have the same topology but different weights, as do N_3 and N_4 .

V	s_1^I	s_1^O	s_2^I	s_2^O	s_3^I	s_3^O	s_4^I	s_4^O
a	396	6	396	200	350	200	350	396
b	8	400	8	400	202	100	398	100
c	4	0	392	0	398	300	398	300
d	8	400	8	400	100	200	100	200
e	396	6	396	200	150	400	150	400
Mean		162.4		240		240		279.2

Table 2: In-strength s_k^I and out-strength s_k^O for each example $k = 1, \dots, 4$.

We classify the nodes as large or small with respect to the average values of the corresponding centrality measure. Table 2 shows that in network

N_1 , nodes a and e are large receivers but small spreaders, whereas nodes b and d are small receivers and large spreaders, and node c is peripheral. In network N_2 , the node centrality is the same as that in network N_1 , with the exception of node c, which becomes a large receiver. In network N_3 , nodes of the absorbing class {b, d} are peripheral, and node a is a large receiver but a small spreader; node e is a small receiver but a large spreader, and node c is central. The centralities in network N_4 differ only for node a, which also becomes a large spreader and consequentially a central node; therefore, node b is affected by this variation and becomes a large receiver.

The homogeneous Markov chains related to the networks of the examples share the same state space $V = \{a, b, c, d, e\}$. We denote the Markov chain associated with network N_k by \mathcal{X}_k for $k = 1, \dots, 4$. The transition matrix and the initial probability distribution of \mathcal{X}_k can be obtained from the adjacency matrix \mathbf{W}_k and are labeled as \mathbf{P}_k and $\pi_{0,k}$. Here, we give the transition matrices:

$$\mathbf{P}_1 = \begin{pmatrix} 0 & \bar{0.3} & \bar{0.3} & \bar{0.3} & 0 \\ 0.99 & 0 & 0 & 0.01 & 0 \\ 0 & 0 & 1 & 0 & 0 \\ 0 & 0.01 & 0 & 0 & 0.99 \\ 0 & \bar{0.3} & \bar{0.3} & \bar{0.3} & 0 \end{pmatrix}, \quad \mathbf{P}_2 = \begin{pmatrix} 0 & 0.01 & 0.98 & 0.01 & 0 \\ 0.99 & 0 & 0 & 0.01 & 0 \\ 0 & 0 & 1 & 0 & 0 \\ 0 & 0.01 & 0 & 0 & 0.99 \\ 0 & 0.01 & 0.98 & 0.01 & 0 \end{pmatrix},$$

$$\mathbf{P}_3 = \begin{pmatrix} 0 & 0.01 & 0.99 & 0 & 0 \\ 0 & 0 & 0 & 1 & 0 \\ 0.5 & 0 & 0 & 0 & 0.5 \\ 0 & 1 & 0 & 0 & 0 \\ 0.5 & 0 & 0.5 & 0 & 0 \end{pmatrix}, \quad \mathbf{P}_4 = \begin{pmatrix} 0 & 0.5 & 0.5 & 0 & 0 \\ 0 & 0 & 0 & 1 & 0 \\ 0.5 & 0 & 0 & 0 & 0.5 \\ 0 & 1 & 0 & 0 & 0 \\ 0.5 & 0 & 0.5 & 0 & 0 \end{pmatrix}.$$

The initial probability distributions are proportional to the out-strengths because of Eq. (5), and they are written as follows:

$$\begin{aligned} \pi_{0,1}^\top &= [0.008, 0.493, 0, 0.493, 0.007], \\ \pi_{0,2}^\top &= [0.1\bar{6}, 0.\bar{3}, 0, 0.\bar{3}, 0.1\bar{6}], \\ \pi_{0,3}^\top &= [0.1\bar{6}, 0.08\bar{3}, 0.25, 0.1\bar{6}, 0.\bar{3}], \\ \pi_{0,4}^\top &= [0.284, 0.072, 0.215, 0.143, 0.287]. \end{aligned}$$

For illustration, see the Supplementary material, where we present the direct computation of \mathbf{E}_h , for $h = 1, 2, 3$ along with some comments for the case of network N_4 .

The states of the Markov chains \mathcal{X} are easily classified: state c is an absorbing state for Markov chains \mathcal{X}_1 and \mathcal{X}_2 , and the set of states {b, d} is an absorbing class for \mathcal{X}_3 and \mathcal{X}_4 . In accordance with the related networks, the

probabilities of being absorbed by states c and $\{b, d\}$ represent the elements distinguishing \mathcal{X}_1 from \mathcal{X}_2 and distinguishing \mathcal{X}_3 from \mathcal{X}_4 , respectively.

h	N_1	N_2	N_3	N_4
1	0.7718	0.0828	0.5404	0.5503
2	-0.7664	-0.0739	0.5204	-0.0309
3	0.6031	0.0507	0.3515	0.2663
4	-0.6031	-0.0470	0.5067	-0.0130
5	0.5086	0.0361	0.4034	0.1688
...
9996	0	0	-0.0098	-0.0718
9997	0	0	0.0098	0.0718
9998	0	0	-0.0098	-0.0718
9999	0	0	0.0098	0.0718
10000	0	0	-0.0098	-0.0718

Table 3: First and last evaluated values of r_h^{OI} for the four illustrative examples.

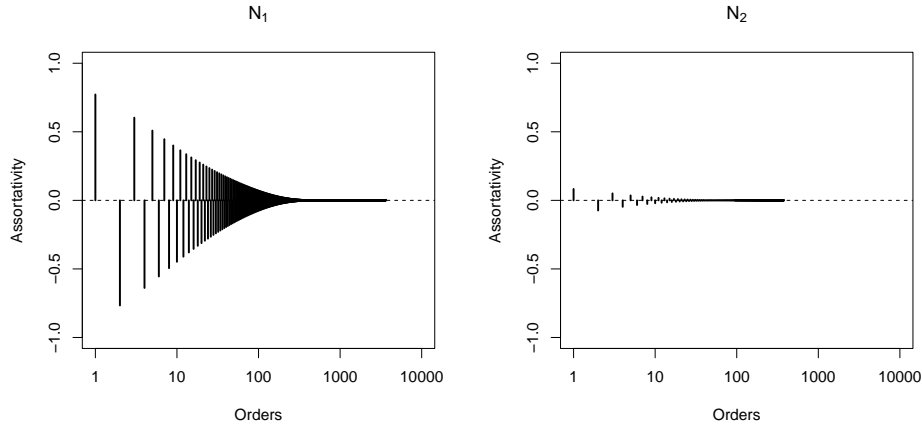


Figure 9: Higher-order assortativity r_h^{OI} between out-strength and in-strength using weighted adjacency matrix to evaluate transition probabilities. The results refer to networks N_1 (left) and N_2 (right). The horizontal axis represents the walk length on a logarithmic scale, and the vertical axis represents the assortativity index.

Next, we inspect the assortativity as the correlation between the out-strength and in-strength associated with the states of the aforementioned Markov chains. Fig. 9 reports the out-in higher-order assortativity r_h^{OI} for

networks N_1 and N_2 . In N_1 , the probability of falling into the absorbing state c is small, so we can consider its effect as marginal. Nodes a and e have small out-strength and high in-strength, in contrast to nodes b and d , which have the opposite characteristics. We identify the pair $\{a, e\}$ as group 1 and the pair $\{b, d\}$ as group 2. At the first step ($h = 1$), the assortativity is due mainly to the correlation between the out-strengths in group 1 and the in-strengths in group 2, and vice versa. As can be seen, there is concordance between them, and therefore positive assortativity. After two steps ($h = 2$), if the Markov chain starts from group 1, then it is highly probable that it jumps to group 2 and then back to group 1, generating disassortative behavior; the same is true if the Markov chain starts from group 2. Consequently, for increasing h , this creates the alternating between positive and negative assortativity for odd and even values of h , respectively, as confirmed in Table 3. The asymptotic zero-assortative behavior is caused by both the randomness and the presence of the absorbing state c . In network N_2 , the same behavior can be observed with a smaller oscillation; this is due to the increased out-degrees of nodes in group 1 and the higher probability of falling into the absorbing state c where there is no centrality variability.

Note that even if there is no variability of strength measures in the sink, there is no indeterminate form in Eq. (1) because the probability of falling into the sink is less than one. Moreover, in network N_1 , the probability of falling into the sink is high, so the asymptotic value is reached immediately. By contrast, in network N_2 the asymptotic value is reached after a long time alternating between assortative and disassortative behavior.

Fig. 10 shows the same results for networks N_3 and N_4 . These networks are characterized by the absorbing class $\{b, d\}$ and the complementary one $\{a, c, e\}$ connected by the bridge represented by the edge from node a to node b . Both classes have positive assortativity. In N_3 , the bridge has a low weight, so the inter-assortative behavior dominates. In network N_4 , the weight of the bridge is very high, and so the larger oscillations are justified by the differences between the classes.

8. Conclusions

This paper fills a gap in the literature on complex networks by introducing the concept of higher-order assortativity for weighted and directed networks, where the considered nodal attributes are the directed versions of degree and strength centrality. These measures have a clear interpretation in socioeconomic applications that are well-linked to directed and weighted networks, such as migration and international trade as studied in the proposed

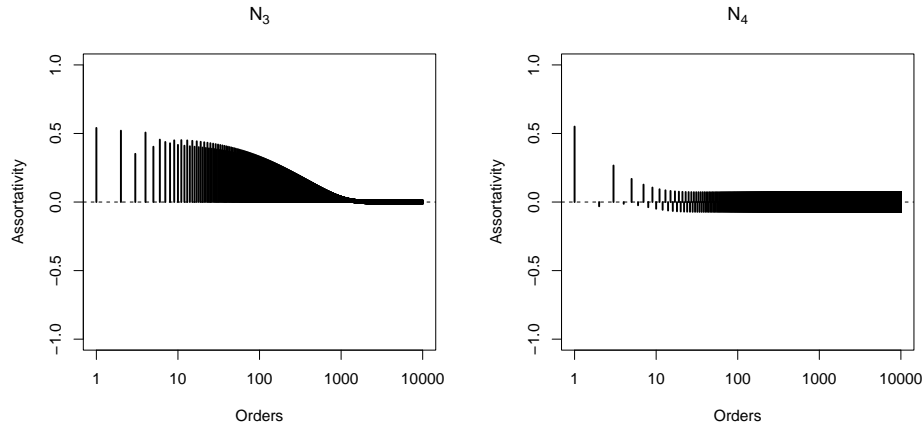


Figure 10: Higher-order assortativity r_h^{OI} between out-strength and in-strength using weighted adjacency matrix to evaluate transition probabilities. The results refer to networks N_3 (left) and N_4 (right). The horizontal axis represents the walk length on a logarithmic scale, and the vertical axis represents the assortativity index.

empirical applications. Furthermore, we also highlighted the strong connection between the introduced assortativity measure and the autocorrelations of suitably defined Markov chains.

The versatility of the proposed methodology makes it possible to describe the preferential attachment of a wide set of models, with a possible paradigmatic empirical instance being the structure and systemic risk profile of the interbank system (Bo and Capponi, 2015; Castellano et al., 2021; Castiglionesi and Eболи, 2018; Cerqueti et al., 2022, 2021; Bargigli et al., 2015). Moreover, the interpretability of the proposed assortativity measure in the context of Markov chains might be exploited efficiently to analyze the properties of some classes of dynamical random systems that have Markovian properties. In this respect, it is important to note that the decay of the autocorrelation explains the long-term memory properties of the underlying stochastic process (Hurst, 1951). These challenging themes are already part of our research agenda.

References

Acemoglu, D., Akcigit, U., Kerr, W., 2016. Networks and the macroeconomy: An empirical exploration. *Nber macroeconomics annual* 30, 273–335.

- Acemoglu, D., Carvalho, V.M., Ozdaglar, A., Tahbaz-Salehi, A., 2012. The network origins of aggregate fluctuations. *Econometrica* 80, 1977–2016.
- Antonietti, R., Falbo, P., Fontini, F., Grassi, R., Rizzini, G., 2022. The world trade network: country centrality and the covid-19 pandemic. *Applied Network Science* 7, 18.
- Arcagni, A., Grassi, R., Stefani, S., Torriero, A., 2017. Higher-order assortativity in complex networks. *European Journal of Operational Research* 262, 708–719.
- Arcagni, A., Grassi, R., Stefani, S., Torriero, A., 2019. Extending assortativity: An application to weighted social networks. *Journal of Business Research* .
- Bang-Jensen, J., Gutin, G.Z., 2008. *Digraphs: theory, algorithms and applications*. Springer Science & Business Media.
- Bargigli, L., Di Iasio, G., Infante, L., Lillo, F., Pierobon, F., 2015. The multiplex structure of interbank networks. *Quantitative Finance* 15, 673–691.
- Barigozzi, M., Fagiolo, G., Garlaschelli, D., 2010. Multinetwork of international trade: A commodity-specific analysis. *Phys. Rev. E* 81, 046104.
- Bartesaghi, P., Clemente, G.P., Grassi, R., Luu, D.T., 2022. The multilayer architecture of the global input-output network and its properties. *Journal of Economic Behavior & Organization* 204, 304–341.
- Bhattacharya, K., Mukherjee, G., Saramäki, J., Kaski, K., Manna, S.S., 2008. The international trade network: weighted network analysis and modelling. *Journal of Statistical Mechanics: Theory and Experiment* 2008, P02002.
- Bick, C., Gross, E., Harrington, H.A., Schaub, M.T., 2023. What are higher-order networks? *SIAM Review* 65, 686–731.
- Bo, L., Capponi, A., 2015. Systemic risk in interbanking networks. *SIAM Journal on Financial Mathematics* 6, 386–424.
- Breza, E., Chandrasekhar, A., Golub, B., Parvathaneni, A., 2019. Networks in economic development. *Oxford Review of Economic Policy* 35, 678–721.

- Burstein, A., Kurz, C., Tesar, L., 2008. Trade, production sharing, and the international transmission of business cycles. *Journal of Monetary Economics* 55, 775–795.
- Carvalho, V.M., 2014. From micro to macro via production networks. *Journal of Economic Perspectives* 28, 23–48.
- Carvalho, V.M., Tahbaz-Salehi, A., 2019. Production networks: A primer. *Annual Review of Economics* 11, 635–663.
- Castellano, R., Cerqueti, R., Clemente, G.P., Grassi, R., 2021. An optimization model for minimizing systemic risk. *Mathematics and Financial Economics* 15, 103–129.
- Castiglionesi, F., Eboli, M., 2018. Liquidity flows in interbank networks. *Review of Finance* 22, 1291–1334.
- Cerqueti, R., Cinelli, M., Ferraro, G., Iovanella, A., 2022. Financial interbanking networks resilience under shocks propagation. *Annals of Operations Research* <https://doi.org/10.1007/s10479-022-04567-w>.
- Cerqueti, R., Clemente, G.P., Grassi, R., 2021. Systemic risk assessment through high order clustering coefficient. *Annals of Operations Research* 299, 1165–1187.
- Csardi, G., Nepusz, T., 2006. The igraph software package for complex network research. *InterJournal Complex Systems*, 1695. URL: <https://igraph.org>.
- Csárdi, G., Nepusz, T., Traag, V., Horvát, S., Zanini, F., Noom, D., Müller, K., 2023. igraph: Network Analysis and Visualization in R. URL: <https://CRAN.R-project.org/package=igraph>, doi:10.5281/zenodo.7682609. r package version 1.5.0.
- De Benedictis, L., Nenci, S., Santoni, G., Tajoli, L., Vicarelli, C., 2014. Network analysis of world trade using the baci-cepii dataset. *Global Economy Journal* 14, 287–343.
- De Benedictis, L., Tajoli, L., 2011. The world trade network. *The World Economy* 34, 1417–1454.
- Di Silvestre, M.L., Ippolito, M.G., Sanseverino, E.R., Sciumè, G., Vasile, A., 2021. Energy self-consumers and renewable energy communities in italy: New actors of the electric power systems. *Renewable and Sustainable Energy Reviews* 151, 111565.

- D’Arcangelis, A.M., Rotundo, G., 2016. Complex networks in finance. *Complex Networks and Dynamics: Social and Economic Interactions*, 209–235.
- Estrada, E., Hatano, N., Gutierrez, A., 2008. “Clumpiness” mixing in complex networks. *Journal of Statistical Mechanics: Theory and Experiment*, P03008.
- Fagiolo, G., Mastrorillo, M., 2013. International migration network: Topology and modeling. *Phys. Rev. E* 88, 012812.
- Fagiolo, G., Reyes, J., Schiavo, S., 2008. On the topological properties of the world trade web: A weighted network analysis. *Physica A: Statistical Mechanics and its Applications* 387, 3868–3873. *Applications of Physics in Financial Analysis*.
- Foster, J.G., Foster, D.V., Grassberger, P., Paczuski, M., 2010. Edge direction and the structure of networks. *Proceedings of the National Academy of Sciences* 107, 10815–10820.
- Garlaschelli, D., Loffredo, M.I., 2004. Fitness-dependent topological properties of the world trade web. *Physical review letters* 93, 188701.
- Garlaschelli, D., Loffredo, M.I., 2005. Structure and evolution of the world trade network. *Physica A: Statistical Mechanics and its Applications* 355, 138–144.
- Gómez, S., Arenas, A., Borge-Holthoefer, J., Meloni, S., Moreno, Y., 2010. Discrete-time markov chain approach to contact-based disease spreading in complex networks. *EPL (Europhysics Letters)* 89, 38009.
- Gosak, M., Milojević, M., Duh, M., Skok, K., Perc, M., 2022. Networks behind the morphology and structural design of living systems. *Physics of Life Reviews* 41, 1–21.
- Gross, J.L., Yellen, J., 2003. *Handbook of graph theory*. CRC press.
- Hurst, H.E., 1951. Long-term storage capacity of reservoirs. *Transactions of the American society of civil engineers* 116, 770–799.
- Iannelli, F., Koher, A., Brockmann, D., Hövel, P., Sokolov, I.M., 2017. Effective distances for epidemics spreading on complex networks. *Physical Review E* 95, 012313.
- Leung, C., Chau, H., 2007. Weighted assortative and disassortative networks model. *Physica A: Statistical Mechanics and its Applications* 378, 591–602.

- Long, J.B., Plosser, C.I., 1983. Real business cycles. *Journal of Political Economy* 91, 39–69.
- Majhi, S., Perc, M., Ghosh, D., 2022. Dynamics on higher-order networks: A review. *Journal of the Royal Society Interface* 19, 20220043.
- Mayo, M., Abdelzaher, A., Ghosh, P., 2015. Long-range degree correlations in complex networks. *Computational Social Networks* 2, 1–13. doi:10.1186/s40649-015-0011-x.
- Meghanathan, N., 2016. Assortativity analysis of real-world network graphs based on centrality metrics. *Computer and Information Science* 9, 7–25.
- Mundt, P., 2021. The formation of input–output architecture: Evidence from the european union. *Journal of Economic Behavior & Organization* 183, 89–104.
- Newman, M., 2010. *Networks: an introduction*. Oxford university press.
- Newman, M.E.J., 2002. Assortative Mixing in Networks. *Physical Review Letters* 89, 208701. doi:10.1103/PhysRevLett.89.208701.
- Noldus, R., Van Mieghem, P., 2015. Assortativity in complex networks. *Journal of Complex Networks* 3, 507–542.
- Norris, J.R., Norris, J.R., Norris, J.R., 1998. Markov chains. Number 2 in *Cambridge Series in Statistical and Probabilistic Mathematics*, Cambridge University Press.
- OECD, 2020. International migration database.
- Piraveenan, M., Prokopenko, M., Zomaya, A., 2010. Assortative mixing in directed biological networks. *IEEE/ACM Transactions on computational biology and bioinformatics* 9, 66–78.
- Serrano, M., Boguñá, M., Vespignani, A., 2007. Patterns of dominant flows in the world trade web. *Journal of Economic Interaction and Coordination* 2, 111–124.
- UN COMTRADE, 2022. International trade statistics database. Data retrieved from International Trade Statistics Database, <https://comtrade.un.org/>.

- Van Mieghem, P., Wang, H., Ge, X., Tang, S., Kuipers, F.A., 2010. Influence of assortativity and degree-preserving rewiring on the spectra of networks. *The European Physical Journal B* 76, 643–652. doi:10.1140/epjb/e2010-00219-x.
- Varela, L.M., Rotundo, G., 2016. Complex network analysis and nonlinear dynamics. *Complex Networks and Dynamics: Social and Economic Interactions* , 3–25.
- Yuan, Y., Yan, J., Zhang, P., 2021. Assortativity measures for weighted and directed networks. *Journal of Complex Networks* 9, cnab017.